Volume 1 | Number 1 | Jan 2013 | Pages 1–100

Journal of
Materials Chemistry A

Materials for energy and sustainability
www.rsc.org/materialsA

Li⁺

ROYAL SOCIETY
OF CHEMISTRY

ROYAL SOCIETY
OF CHEMISTRY

www.rsc.org/materialsA

PAPER

Inkjet printing of self-healing polymers for enhanced composite interlaminar properties

Elliot J. Fleet[a], Yi Zhang[b] Simon A. Hayes[a] and Patrick J. Smith*[b]

Inkjet printing has been used to introduce an organic system that demonstrates thermally activated self-healing in composites. The organic system is composed of monomers that, when polymerised, are capable of thermally activated self-healing through a reversible Diels-Alder mechanism. After being synthesised the monomers were formulated into inks and inkjet printed on to carbon fibre epoxy prepreg. The
10 polymers were co-cured with the prepreg into composite laminates and the effect on the interlaminar properties of the resultant system was investigated. A single ply at the mid-plane of double cantilever beam specimens was shown to increase the initiation (by NL Point) of the interlaminar fracture toughness by 9%. The interlaminar fracture toughness with regards to crack propagation was shown to increase further by up to 27%. Increases in apparent interlaminar shear strength as measured by short beam shear
15 of up to 11% were also observed compared to unprinted controls. After a thermal treatment the short beam shear specimens are retested and the printed specimens are shown to have significantly smaller decreases in properties compared to the control which is consistent with repair in the interlaminar region.

Introduction

Polymer composite materials have been produced now for over
20 half a century with the first 'fibreglass' materials produced in the 1940s. A polymer composite material consists of reinforcements within a polymer matrix. The components are not dissolved, they remain separate although are bound together and so act cooperatively. Composite materials are well known for their high
25 specific strength and stiffness along with their excellent fatigue resistance.

The light weight of polymer composites compared to the incumbent materials gives clear financial and environmental benefits when used in sectors such as aerospace, automotive and
30 mass transport in the form of fuel savings and corresponding reductions in CO_2 emissions.

Composite materials were first introduced in part into commercial aircraft in the 1950s and since this time the proportion used has been growing. Today, modern aircraft such
35 as Boeing's 787 Dreamliner and Airbus' A350XWB are made up of over 50% composite by weight (which corresponds to around 80% by volume).

There are concerns, however, regarding the inferior fracture toughness of the majority of composite parts compared to
40 their metallic competitors and the difficulty detecting and assessing hidden damage within composites which is often hidden or barely visible within the structure. This has led to a large amount of research effort in non-destructive testing and self-sensing in composites [1-6].
45 When a composite is damaged this often results in

delamination in which the bonding between plies is compromised; this leads to a large decrease in properties. Delamination is said to represent the weakest failure mode in composite materials [7]; therefore interlaminar toughening or
50 lifetime enhancement by self-healing is of great interest.

Current approaches to improving susceptibility to delamination include thermoplastic toughening of the bulk resin or interface and three-dimensional reinforcements as opposed to the more traditional lamellar arrangement. These approaches are successful
55 but often they are at the detriment of other properties such as strength or stiffness.

Inkjet Printing (IJP) is a flexible, precise material deposition technique which is historically widely used for graphical printing. While graphical applications are still important; IJP is also
60 increasingly gaining popularity as a patterning technique in a variety of technical fields such as printed electronics [8], conductors [9] and RFID tags [10] or tissue engineering [11]. Printable materials can be organic or inorganic, in solution or as nanoparticle suspensions such as silver nanoparticles used to
65 produce conductive paths. The main limitation is the ink viscosity which should be no higher than approximately 20 cP.

Advantages of IJP involve the precise control of the deposition of small amounts of material with minimal waste and without the need for masks such as those used in photo lithography or screen
70 printing. Another advantage is that additional print-heads can be added to a system making scale-up to mass production relatively simple. The non-contact nature of IJP allows a wide variety of substrates to be used including, as shown recently [12,13], carbon

This journal is © The Royal Society of Chemistry 2014

J. Mater. Chem. A, 2014, **[vol]**, 00–00 | **1**

fibre pre-impregnated with epoxy resin (prepreg).

In this manuscript, monomers capable of thermally reversible cross-linking through Diels-Alder chemistry are synthesised. The monomers are formulated into ink solutions and printed as droplets in a hexagonal array onto the prepreg layers. This prepreg is used to manufacture carbon-fibre epoxy specimens using a typical vacuum bagging oven cure schedule with the monomers cured *in situ* with the composite. The interlaminar properties of the resulting composites are then studied along with the effect of a thermal treatment designed to extend lifetime by self-healing of interlaminar microcracks.

Thermally reversible polymers were selected for this novel application for several reasons. The first reason is that the reversibility of polymers based on main chain or pendant Diels-Alder moieties is well established in the literature [14-17]. Secondly, thermally reversible covalent bonding is a useful approach to self-healing polymers as it does not rely on liquid resin delivery through microencapsulated systems [18] or embedded fibres [19]; such approaches have inherent lifetime concerns or the potential to compromise mechanical performance.

The other side of the argument is that using such specialist polymers as a matrix may have prohibitive costs as they are not presently produced in a large scale. In addition thermally activated healing requires external intervention and would require an active self-sensing system [20, 21] or a thermal treatment built into the periodic maintenance of the part.

This approach circumvents most of the technical and economical problems by applying extremely small amounts of material directly to the interlaminar region where it is most needed. Advantages of an additive system include lower costs, established performance, easier certification and acceptance in the market compared to the development of a completely new matrix system.

Experimental

The production and testing of the inkjet modified composites required several steps. First, Thiele's acid, a common intermediate for the monomers, was synthesised. The Thiele's acid was used to synthesise two monomers referred to as "Monomer 400" and "Monomer 401". The naming system is taken from the paper in which their synthesis was first presented [22]; the number refers to the number of carbon, nitrogen and oxygen atoms in the diol-based section.

The monomers were then formulated into printable inks and selectively deposited onto layers of prepreg using inkjet printing. The modified prepreg was then used to manufacture test specimens using hand lay-up and oven cured under vacuum.

Materials

Dicyclopentadiene (DCPD, 95%, BHT stabilized) was purchased from Alfa Aesar, Heysham, UK and was used as supplied. The sodium metal (99%, large lumps in kerosene) was supplied by Sigma Aldrich, Gillingham, UK; the metal was cut into smaller pieces and washed with light petroleum before use. The pyridine (99.8%, anhydrous) was supplied by Sigma Aldrich, in a sure-seal bottle and used as received. The thionyl chloride (97%) was supplied by VWR, East Grinstead, UK and used as received. The 1,4-butane diol (99%) was supplied by Sigma Aldrich and was

distilled from (and stored over) 4Å molecular sieves. The diethylene glycol (98%) was supplied by VWR and used as received. All other reagents were supplied by Sigma Aldrich and were at least 99% purity.

All solvents were supplied by VWR or Fisher Scientific, Loughborough, UK and were at least 99% purity. Where solvents are described as 'dried' this was done using a drying column consisting of an activated alumina/copper catalyst and inert nitrogen atmosphere. The water content for the dried tetrahydrofuran was determined to be 13-14 ppm by Karl-Fischer titration. All other dried solvents had a water content of <10 ppm.

All the synthesis work presented in this paper was done under inert nitrogen (BOC Special Products, 99.998 %) that had been further purified by passing through a Model 1000 oxygen scavenger column (Chromatography Research Supplies, Louisville, KY, USA).

The commercial aerospace grade toughened unidirectional epoxy-carbon prepreg system Cycom 977-2 was supplied by Cytec Industries Inc, Östringen, DE. The prepreg was less than two years old, stored sealed at -18 °C with an out-life less than the maximum number recommended by the manufacturer (40 days). The prepreg was allowed to warm to room temperature in its sealed packet for a minimum of 24 hours before use.

Synthesis of Thiele's acid

The synthesis of Thiele's acid has been modified from that presented by Murphey *et al.* [22] and has more in common with earlier synthetic approaches [23, 24]; the reason for this is that these earlier routes are more suitable to standard manifold manipulations with nitrogen as an inert gas. Dicyclopentadiene (DCPD) (approx 150 ml) was cracked into cyclopentadiene (CPD) using a reactive distillation setup; refluxing the DCPD (~170 °C) and recovering the lower boiling point CPD in an ice-cooled flask.

Sodium pieces (10 g, 0.43 mol) were transformed into a high surface area 'sand' by refluxing with rapid stirring in dried toluene (250 ml). The stirring was stopped and the mixture was allowed to cool before the toluene was removed by syringe and the sodium was washed with two 25 ml portions of dry tetrahydrofuran (THF) which were subsequently removed by syringe and discarded. Dry THF (500 ml) was added to the sodium and with gentle stirring 50 ml of CPD was added drop wise over the course of *ca.* 4 hours; this forms a pink / pale red concentrated sodium cyclopentadienyl (NaCP) solution with the evolution of hydrogen gas.

When the sodium is completely consumed a slurry of dry ice (1 kg) in THF (500 ml) was produced in a large (2 L) Erlenmeyer flask into which 50 ml portions of the THF/NaCP were quickly transferred with a syringe. The dry ice was allowed to sublime overnight after which the solution was concentrated, leaving a solid white residue.

The residue was dissolved in deionised water (500 ml) and washed with three (100 ml) portions of dichloromethane (DCM). The aqueous layer was acidified using drop wise addition of 10% hydrochloric acid and the precipitate was removed by vacuum filtration and washed with deionised water (3 x 100 ml portions). This crude product was recystallised from methanol and dried under vacuum at 50 °C overnight to yield white solid Thiele's Acid (30.60 g, 0.14 mol, 64% yield based on Na, mp 210-212

°C). ^{1}H NMR (400 MHz, d-DMSO): δ 1.36 (d, J = 8.5 Hz, 1 H), 1.54 (d, J = 8.5 Hz, 1 H), 1.90 (d, J = 18.0 Hz, 1 H), 2.30 (dd, J = 18.0, 10.4 Hz, 1 H), 2.88 (m, 1 H), 3.10 (s, 1 H), 3.18 (s, 1 H), 3.47 (m, 1 H), 6.40 (s, 1 H), 6.74 (s, 1 H), 12.50 ppm (s, 2H).
^{13}C NMR (400 MHz, d-DMSO): δ 33.13 (CH_2), 40.68 (CH), 40.54 (CH), 47.28 (CH), 50.57 (CH_2), 54.26 (CH), 138.61 (>C=), 139.51 (>C=), 142.91 (CH), 147.29 (CH), 166.12 (C=O), 166.38 (C=O) ppm.

Synthesis of Thiele's acid chloride

Against a dry nitrogen counterflow, Thiele's acid (10.04 g, 46 mmol) was added to a reaction flask, followed by thionyl chloride (300 ml). The open neck was sealed using a septum and the nitrogen flow was lowered. The mixture of Thiele's acid and thionyl chloride was stirred using a magnetic stirrer at room temperature. HCl gas was produced which was captured by passing the gas output through a dilute solution of calcium hydroxide. At the point where the solution had turned transparent and there was no further gas evolution the reaction was deemed to be complete; but an extra 30 minutes was allowed to ensure full conversion. The excess thionyl chloride was recovered using vacuum distillation leaving a viscous brown oil which was directly used in the lactonisation step.

Synthesis of Monomer 400

Pyridine (18 mL, 0.23 mol) and dry THF (500 mL) was added through a septum to a 2.5 L dry, N_2 purged, 3-necked reaction vessel fitted with two pressure equalising dropping funnels (250 ml) and a Graham condenser. Dry THF (100 mL) was added via a septum to the Thiele's acid chloride (46 mmol, assuming the acylation is quantitative) produced in the previous step and stirred using the magnetic stirrer to form a clear brown solution. The solution of Thiele's acid chloride in THF was transferred via cannula through a septum into one of the closed pressure-equalising dropping funnels. To ensure a quantitative transfer; any remaining Thiele's acid chloride was washed into the dropping funnel by repeating the transfer with 2 more batches of 50 ml THF. The dropping funnel was then topped up to 250 mL volume with dry THF.

1,4-butane diol (4.11 g, 46 mmol) in THF was added through the septum to the second closed dropping funnel and topped up to the 250 mL line with more dry THF. The contents of the dropping funnels were added drop-wise at approximately equal rates to the rapidly stirred solution of pyridine in THF. The solution was heated to reflux over the entire addition process (c.a. 5 hours).

After cooling, the solution was concentrated under vacuum and the resulting oily brown solid was washed with 10% aqueous HCl and extracted, three times, with DCM. The organic phase was dried over anhydrous magnesium sulfate, filtered, and concentrated; forming a brown viscous oil which was purified using flash column chromatography (10% diethyl ether in dichloromethane on silica gel) to produce a white crystalline solid Monomer 400 (1.21 g, 4.4 mmol, 9.6% yield for both steps based on Thiele's Acid, mp 83 °C). ^{1}H NMR (400 MHz, CDCL$_3$): δ 1.31 (d, J = 8.5 Hz, 1 H), 1.54 (d, J = 8.5 Hz, 1 H), 1.69-1.95 comp, 4 H), 2.16 (d, J = 20 Hz, 1 H), 2.40 (m, 1 H), 2.83 (m, 1 H), 3.21 (m, 1 H), 3.45-3.62 (comp, 4 H), 4.79 (m, 1 H), 4.92 (m, 1 H), 6.50 (s, 1 H), 6.58 ppm (s, 1 H). ^{13}C NMR (400 MHz,

CDCl$_3$): δ 25.20 (CH_2), 25.93 (CH_2), 33.18 (CH_2), 39.89 (CH), 46.78 (CH_2), 47.24 (CH), 47.84 (CH), 53.37 (CH), 63.62 (CH_2), 64.28 (CH_2), 144.75 (CH), 146.98 (CH) ppm (the quaternary carbons did not resolve on the instrument).

Synthesis of Monomer 401

With the same equipment as described for Monomer 400 in the previous section; pyridine (3.7 ml, 45 mmol) and dry THF (500 ml) were added to the 2.5 L reaction vessel. To this was added drop-wise a solution of Thiele's acid chloride (9.3 mmol) in 250 mL THF simultaneously with a solution of diethylene glycol (0.99 g, 9.3 mmol) in 250 mL THF at approximately equal rates.

After approximately 5 hours the solution was concentrated using the rotary evaporator and the resulting oily brown solid was washed with 10% aqueous HCl and extracted, three times, with DCM. The organic phase was dried over anhydrous magnesium sulfate, filtered, and concentrated; forming a brown viscous oil.

Flash column chromatography was used for purification (20% diethyl ether in dichloromethane on silica gel) to yield Monomer 401, a pale yellow crystalline solid (m.p. 39 °C, 3.64 g, 12.6 mmol, 18.2%)). 1H NMR (400 MHz, CDCl3): δ 1.32 (d, J = 8.5 Hz, 1 H), 1.57 (m, 1 H), 2.19 (m, 1 H), 2.42 (m, 1 H), 2.86 (m, 1 H), 3.25 (m, 1 H), 3.45 (m, 1 H), 3.53 (comp, 2 H), 3.66 (comp, 2 H), 3.75 (comp, 2H), 3.88 (m 1 H), 4.85 (m, 1 H), 4.95 (m, 1 H), 6.52 (s, 1 H), 6.71 ppm (s, 1 H). 13C NMR (400 MHz, CDCl3): δ 33.33 (CH2), 40.27 (CH), 46.88 (CH), 47.63 (CH), 48.00 (CH2), 53.61 (CH), 62.25 (CH2), 62.31 (CH2), 68.30 (CH2), 69.80 (CH2), 136.75 (>C=), 138.00 (>C=), 143.96 (CH), 147.38 (CH), 165.00 (C=O), 165.21 (C=O) ppm.

Formulation of the monomer solutions for printing

Monomer crystals (1.00 g) were added to 20 mL of chloroform or ethyl acetate in a vial. The vial was stoppered and the vessel was shaken gently for c.a. 10 minutes after which time the material was fully dissolved to form a 5% w/v solution. To make the 1% solution 10 mL of the 5% solution prepared above was removed using a volumetric pipette and transferred into a 50 mL volumetric flask. The volumetric flask was filled to the mark using fresh solvent and gently shaken. Both solutions were filtered through cotton-wool in a Pasteur pipette and then through a 0.2 μm syringe filter (Sarstedt, Nümbrecht, DE) into 10 mL vials ready for printing.

Inkjet Printing

Printing was carried out on a Jet-Lab 4 × 1 printing system (Microfab Inc., Texas, USA) equipped with a 60 μm diameter drop-on-demand print-head (MJ-AT-01-60, Microfab Inc.). Ejection of a droplet was achieved by excitation of the printhead with an electrical pulse. Print settings varied but typically this consisted of a 43-45 V pulse of 35 μs duration. The distance between the printhead nozzle and the prepreg was approximately 1 mm. Borosilicate glass microscope slides and carbon-epoxy prepreg were both used as substrates.

Thermal polymerisation of the printed monomers

The glass slides with Monomer 401 print pattern were placed onto a heated plate and the plate temperature was set to 130 °C; this corresponded to approximately 120 °C on the surface of the glass as measured using an infra-red non-contact thermometer.

The heat was maintained for 2 hours after which the heated plate was turned off and the plate and the substrate were allowed to cool to room temperature at a natural rate.

Hot-stage optical microscopy of the monomer pattern

A 20 mm x 20 mm section of a glass slide previously printed with a Monomer 401 print pattern was placed onto a microscope hot stage and heated to 180 °C for 3 hours. A representative printed dot was chosen and photographs were taken before heating, after heating and every subsequent hour to ensure the pattern was robust enough to withstand the prepreg cure temperatures.

Bulk polymer specimen fabrication and DMA testing

DMA testing was undertaken on a Perkin Elmer DMA 8000 instrument equipped with a liquid nitrogen cooling system. An open female mould was produced from built-up layers of PTFE coated adhesive fibreglass mounted on a glass microscope slide. The mould cavity was approximately 20 mm x 5 mm by 3 mm deep. Finely ground monomer was added to the cavity and the Monomer 401 was cured under full vacuum, in a vacuum oven, at 120 °C for 12 hours. Monomer 400 was cured for the same length of time but at 150 °C.

Composite specimen preparation

All laminates were unidirectional, flipped in a symmetric fashion at the mirror plane to reduce strains arising from distortions caused by storage on the prepreg roll. The laminates were consolidated by hand using a blunt plastic tool and the application of gentle heat from a domestic hair-dryer. There were no separate vacuum debulking stages. The laminates were envelope vacuum bagged on a PTFE covered steel tool under perforated PTFE and breather cloth before oven curing at the following schedule:

- Ramp from room temperature to 120 °C at 1 °C min^{-1}
  - Hold at 120 °C for 30 min
- Ramp to 150 °C at 1 °C min^{-1}
  - Hold at 150 °C for 30 min
- Ramp to 180 °C at 1 °C min^{-1}
  - Hold at 180 °C for 195 min
- Ramp to room temperature at 1 °C min^{-1}

The reduced heating rates and additional 150 °C isotherm were used to reduce potential exotherm as the thickness of the laminates required for some of the tests were thicker than the maximum thickness recommended on the prepreg datasheet (2 mm).

Mechanical Testing

The critical energy release rate

The critical energy release rate or interlaminar fracture energy (G_{IC}) was evaluated by means of a double cantilever beam test performed according to BS ISO 15024:2001 :1998 [25]. Six specimens were cut to 125 ± 1 mm x 20 ± 0.5 mm from each 150 mm x 150 mm panel. The panels were fabricated from 12 layers of prepreg with a PTFE starter film laminated inside such that it projects 60 mm into each specimen; this produced a thickness of 3 ± 0.1 mm. For the printed samples, the printed pattern was applied to the upper surface of the central ply only. The specimens were washed and then dried in a vacuum oven at 50 °C for around 2 hours. 12 mm x 12 mm centre-drilled

aluminium blocks were bonded (Araldite standard, Huntsman), to the PTFE-containing specimen ends after light preparation with 240 grit wet and dry paper (used dry). The edges of the specimens were painted with corrector fluid (Tipp-ex) to allow better contrast. The precrack was introduced using mode I opening at 5 mm min^{-1} until the crack had propagated 3 to 5 mm before unloading at 25 mm min^{-1} and reloading at 5 mm min^{-1}. The crack growth was recorded using an HD video camcorder (Panasonic HC-X900) manually focussed on the edge of the specimen recorded at 1080p and 60 fps and the crack length was measured using frame-by-frame image analysis. The experiment was stopped when the crack reached between 5 to 10 mm from the end of the specimen.

After testing, once the load was removed the double cantilever beam specimens were taped shut using high temperature tape. The specimens were then enclosed in a vacuum bag and heated at 180 °C for 6 hours with a heating and cooling rate of 2 °C min^{-1} under the pressure exerted by the atmospheric pressure on the vacuum bag. After the healing cycle it was necessary to re-bond the end blocks because the high temperature had degraded the adhesive bond. The high temperature tape was left in place until the specimens were re-mounted in the testing machine in order to prevent premature damage before testing. When the specimens were mounted the tape was cut using a scalpel blade.

The interlaminar shear strength

The apparent interlaminar shear strength of the composite samples were evaluated by short beam shear according to BS EN ISO 14130:1998 [26]. Ten specimens of 20 ± 1 mm x 10 ± 0.2 mm were cut from each 120 mm x 60 mm panel. Each panel consisted of 8 layers of prepreg which produced a thickness of 2 ± 0.2 mm. For the 5% printed samples, the printed pattern was applied to the middle four layers. For the 1% printed sample the printed pattern was applied to all layers.

The test was carried out using the preferred specimen geometry and a crosshead speed of 1 mm min^{-1} using a pre-load of 2 N and the displacement taken from the crosshead. In order to prevent complete destruction of the specimens the test was stopped at the point that the load dropped to 5% of the maximum.

Only the specimens that appeared to fail in single or multiple shear were used to calculate the apparent interlaminar shear strength. Specimens that failed in tension or compression or mixed modes were discarded. The specimens that failed in an acceptable shear mode (typically 6 to 8) were retained for a thermal healing treatment (180 °C, 6 hours). After healing they were re-tested in the same orientation as they were initially tested.

Results and Discussion

Monomer Synthesis

The monomers selected for this study were first presented by Murphey et. al. [22] along with data related to the bulk polymers and their intrinsic thermal repair mechanism. The modified scheme used in this work is shown in Scheme 1. At its heart lies the dicylopentadiene (DCPD, Structure **1**) functional unit which exists in thermal equilibrium with two equivalents of cyclopentadiene (CPD). The reduction of CPD with elemental sodium produces a reactive cyclopentadienyl ion (Structure **2**).

Upon quenching with electrophilic CO_2 and acid workup and a minor electric rearrangement [23] the major product is produced, a dimeric carboxylic acid (Structure **3**, 3a,4,7,7a-tetrahydro-4,7-methano-1H-indene-2,6-dicarboxylic acid) known as Thiele's acid after the first person to synthesise it [27]. The acyl chloride

derivative of Thiele's acid, Structure **4**, is formed using a standard transformation with thionyl chloride and a lactone ring is formed by nucleophilic substitutions with a diol or glycol in the presence of pyridine.
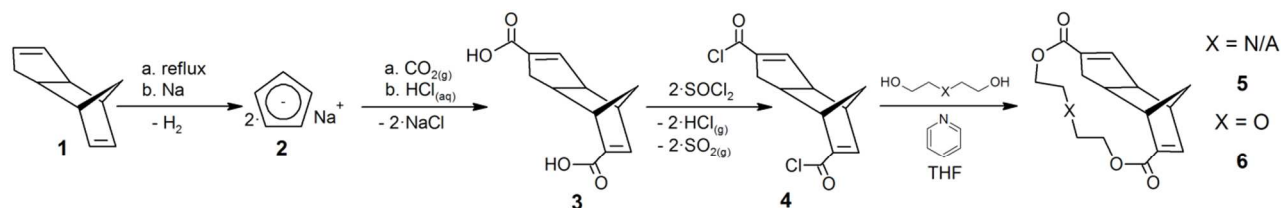
Scheme 1 The synthesis route for production of the monomers used for ink formulation

The final step proved problematic as the side products of this reaction are mixtures of oligomers from the intermolecular products that are sparingly soluble and thus difficult to purify. The yields obtained, however, were sufficient to test the monomers as printable additives. Using the naming scheme suggested by Murpey et. al. based on the number of carbon, nitrogen and oxygen atoms in the lactone tether two monomers were produced depending on which diol or glycol was used. Use of 1,4-butane diol results in "Monomer 400" (Structure **5**) and use of diethylene glycol produces "Monomer 401" (Structure **6**).

Monomer Inkjet Printing

Initially chloroform was chosen as a solvent; the reason for this was it was known to be a good solvent for the monomers from the synthetic work undertaken. Prior to the optimisation there were many satellite droplets or undesirable droplet elongations. The formation of the satellite droplets was not ideal as it has an effect on printing quality; however in this case it was not deemed to be a critical problem for this application as the printing is being used as a method of regular material deposition (sandwiched between prepreg plies) rather than for the production of features. After optimisation of the printing parameters, the monomer solutions in chloroform formed relatively stable droplets. It was found, however, that attempts to print monomers with a higher concentration than 1% w/v in chloroform led to blocked printheads after only one or two minutes of printing.

This nozzle clogging behaviour was attributed to the high volatility of chloroform (vapour pressure 21 kPa [28]) leading to solvent evaporation in the print-head. In an attempt to cure this behaviour 10% acetophenone (vapour pressure 0.05 kPa [29]) was added to the 5% w/v inks but there did not appear to be any

noticeable improvement as the printheads were still getting blocked. In order to deposit larger concentrations of monomer an alternative printable solvent had to be found in which the monomers are sufficiently soluble. Solubility parameter modelling and small scale solubility tests indicated the following good solvents for the monomers: Acetone, Tetrahydrofuran, Dichloromethane, Chloroform, Toluene and Ethyl Acetate.

The most important intrinsic physical properties that affect the printability of a given ink are its viscosity (η), density (ρ) and surface tension (γ). The properties can be used with information about the print head nozzle diameter to predict the printability of a given system by calculating using a dimensionless 'Z' number [30, 31], the value of which estimates whether a stable droplet is achievable. The physical properties of these solvents relevant to inkjet printing are shown in Table 1 along with their calculated 'Z' numbers. As the monomers that are being dissolved are relatively low molecular weight and low concentrations it is sufficient to consider the properties of the solvents alone when considering printability.

A printable range of Z values was determined to be between 1 and 10 by Reis and Derby in 2000 [32] using computational fluid dynamics and an experimental study in parallel. Reis and Derby state that the upper limit of Z exists because of the tendency for satellite droplets to form instead of a single stable droplet, and that the lower limit of Z exists because the fluid viscosity dissipates the applied pressure pulse. This is not an absolute range as it has been shown that inks outside this range can be perfectly printable [33, 34], however as a broad tool it is useful. In practice the viscosity is the main limiting factor; if it is too high the fluid is too viscous to be printed by inkjet.

Table 1 Possible solvents for ink formulation with physical data and calculated Z numbers [a]

Solvent	Density, ρ (Kg m^{-3})	Vapour Pressure (kPa)	Viscosity, η (mPa s)	Surface tension, γ (nM m^{-1})	Z Number
Tetrahydrofuran	888	17.3	0.61	26.4	61.5
Toluene	867	2.9	0.60	28.5	64.3
Ethyl Acetate	900	10.3	0.45	23.9	79.8
Chloroform	1488	21	0.58	27.2	84.9
Acetone	791	24.1	0.33	23.7	102
Dichloromethane	1326	47.5	0.44	29.0	110

[a] droplet diameter assumed to be the nozzle diameter, 50 μm, data from Ullman's [28]

After careful consideration of the solvent properties it was

decided that acetone and dichloromethane are not likely

candidates due to their extremely high 'Z' numbers and volatility. Tetrahydrofuran was also suspected to be too volatile so the best candidates available were toluene and ethyl acetate. The inks prepared using ethyl acetate as a solvent proved to be highly
5 successful for printing higher concentrations (5% w/v) without any print-heads clogging, therefore, as a successful system was identified further trials were not necessity. Despite having a 'Z' number significantly higher (79.8) than the upper limit determined by Reis and Derby (10) it was found that after
10 optimisation, satellite droplets were not a problem.

In order to test that the monomers were being successfully deposited by the printing process, Monomer 401 was printed onto a glass microscope slide. Optical microscopy of the pattern obtained showed the intended array was successfully printed. The
15 pattern was regular and repeatable with few misplaced droplets. The diameters of the printed dots varied between about 100 and 120 μm.

The dots, as-printed, could be smeared across the surface by a soft cloth but after cure at 120 ° C for 2 hours the pattern had
20 hardened (presumably through cure of the monomer) and adhered strongly to the glass substrate as they could not be dislodged even with a needle tip. The Monomer 401 pattern was also analysed by hot-stage optical microscopy in which the dot was heated to 180 ° C (to simulate the cure conditions of the epoxy pre-preg).
25 The hot stage microscopy showed the printed dot remained in the same position after thermal treatment with no significant spreading or coalescence prior to complete cure.

The monomer inks were successfully printed onto carbon fibre-epoxy prepreg. Although, the printed pattern on the surface
30 of the prepreg is visible with the naked eye it has not been possible to capture this with a photograph. Glass substrates are more suitable for printing characterisation because they are very smooth, chemically inert and optically transparent so the printed droplets can be observed. It is very difficult to see patterning on
35 prepreg with optical microscopy, however this has been studied for printed thermoplastics on an identical prepreg substrate after adding fluorescent dye. In this study the printed material was shown to remain on the prepreg after a thermal treatment although there was some preferential flow along the fibre
40 direction [12]. It is thought that the surface roughness of prepreg is likely to lead to decreased spreading compared to a smooth glass surface.

Polymerisation

The thermal polymerisation is thought to proceed as shown in
45 Scheme 2, through a combination of retro-Diels-Alder reactions with forward Diels-Alder reactions with disconnections and reconnections occurring at the DCPD unit. As this reaction is carried out in the bulk rather than dilute solution the presence of other monomer molecules leads to the shift from intramolecular
50 units to intermolecular units. It is this intrinsic ability of the matrix to reorganise its covalent bonds that allows the thermal self-repair functionality.
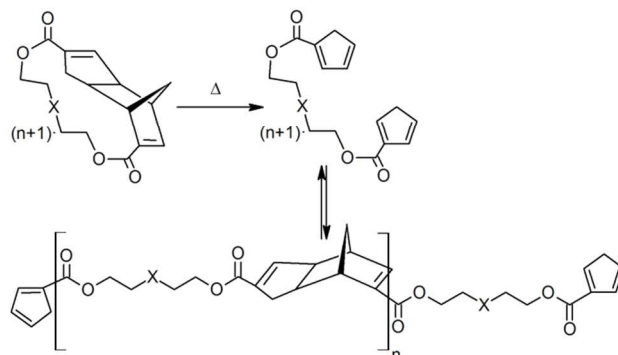
Scheme 2 Part of the thermal polymerisation mechanism showing the
55 formation of the intermolecular dimer connections at the DCPD unit.

Murphey et al. also isolated trimer units formed from the reaction between the Diels-Alder dimer cyclopentene double bond which acts as a dienophile for the reaction of a third
60 cyclopentadiene moiety. The result of this reaction is a fully crosslinked polymer network. There is no reason to expect that the polymerisation chemistry would be changed by the printing of the monomer on a composite substrate.

Dynamic Mechanical Analysis was used to find the glass
65 transition temperatures (T_g) of Polymer 400 and Polymer 401 in bulk specimens. The DMA results are shown in Fig. 1 and Fig. 2. In order to allow thermal repair to occur the polymer chains must be mobile, therefore the temperature must be raised above the Tg.

Glass transitions in polymers are frequency dependent
70 therefore 1 Hz has been chosen as a reference frequency. At 1 Hz Polymer 400 shows the onset in the decrease in storage modulus (E_0') at 100.1 °C, the peak loss modulus (E''_{max}) at 115.6 °C and the peak loss factor (tan δ_{max}) at 131.0 °C. As a glass transition is not a discrete temperature these numbers best outline the range of
75 temperatures over which the transition occurs. E_0' represents the temperature at which the material mechanical properties first start to decrease so is favoured by engineers whereas E''_{max} is represents the point at which the molecules are undergoing the largest change in mobility and is therefore more consistent with
80 values calculated from other methods such as differential scanning calorimetry and is closer to the chemical definition of the glass transition.
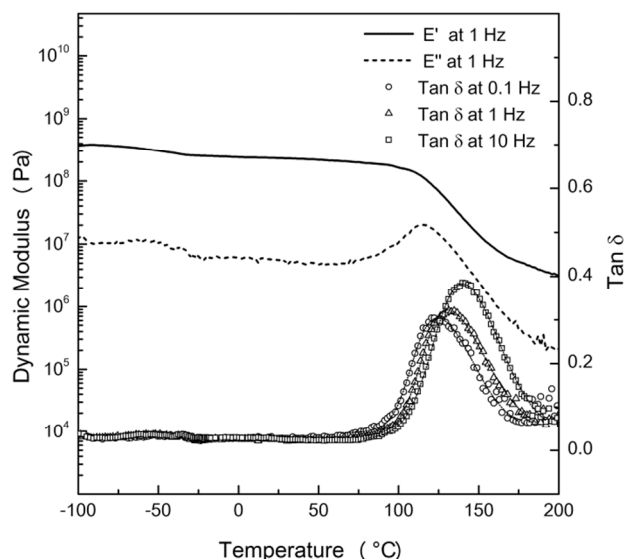
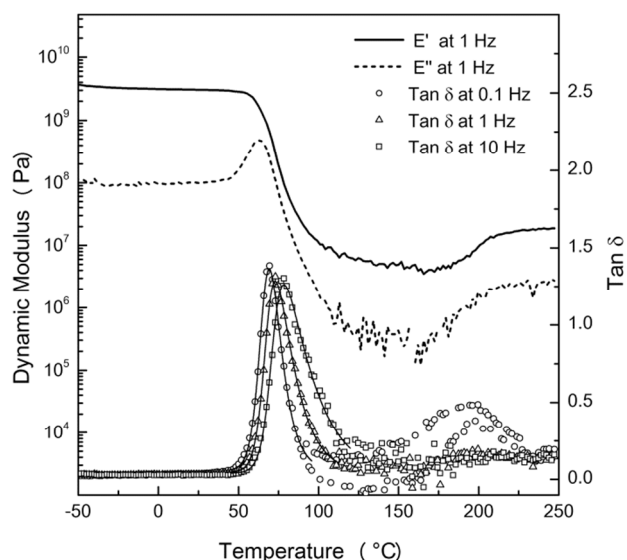Fig. 1 Dynamic mechanical analysis of Polymer 400

Fig. 2 Dynamic mechanical analysis of Polymer 401

5   At 1 Hz Polymer 401 shows the onset in the decrease in storage modulus (E_0') at 55.1 °C, the peak loss modulus (E''_{max}) at 63.4 °C and the peak loss factor (tan δ_{max}) at 73.0 °C. There is evidence of continued cure in this specimen shown by the increase in dynamic moduli at ~175 °C which suggests these
10 values may be low estimates of the glass transition range.

   It is worth noting that because the polymers are being used as interply additives in a carbon-epoxy matrix the glass transition temperatures reported here are not expected to represent the maximum service temperature of the part; the structural
15 performance is borne by the carbon fibres and the epoxy matrix which has a glass transition >180 °C. There may, however, be some influence on the interlaminar properties at high temperatures and this has yet to be investigated.

Composite Testing: Double Cantilever Beam (DCB)

20 Fig. 3 shows typical critical energy release rate (G_{IC}) plots against delamination length obtained from the double cantilever beam experiment for control and printed specimens. The control and 1% printed specimens mostly showed an approximately constant strain energy release rate or a very slight decrease. In some cases
25 (more predominant in the 5% M400 specimen) there were increases in G_{IC} which were sometimes, but not always, followed by a subsequent decrease. This is thought to be caused by fibres bridging between plies which provide additional resistance to mode I delaminations. This is followed by subsequent sharp
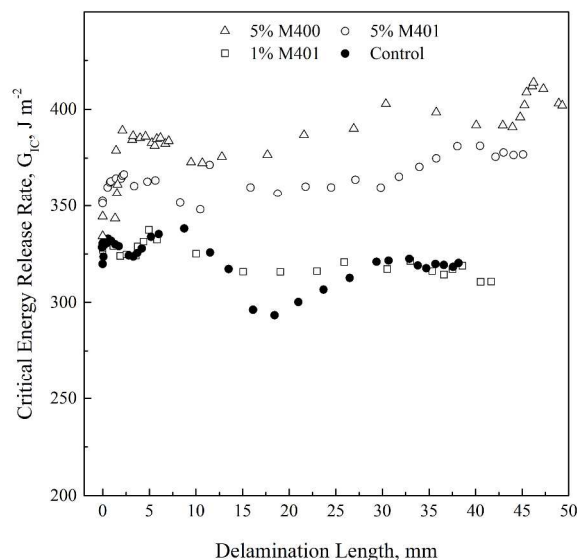30 decrease in G_{IC} if these fibres fail in tension before no additional fibre bridging has occurred.

Fig. 3 Typical critical energy release rate (G_{IC}) plots against delamination length for both printed and unprinted control composite samples
35 (normalised to 0 mm by the position of the starter crack).

Table 2 shows the mean results obtained from the double cantilever beam experiments.

   The NL, VIS and C5%/MAX points are representative measures of critical energy release rate at different points
40 attributed to the initiation of delamination. The NL point refers to the point of deviation from linearity on the load-displacement curve. The VIS point refers to the onset of delamination, as determined by visual observation, in this case the first video frame in which the delamination extends beyond the position of
45 the starter crack. The C5%/MAX point is the intersection on a load-displacement chart between the plotted data and a straight line drawn through the linear portion of the data but modified with an additional 5% compliance or the maximum load (whichever comes first) [25].

50   The propagation (PROP) points are all the points measured after the initiation points. In this work the median of these points has been used for comparison between samples of the propagation of mode I cracks.

PAPER

Table 2 Results from the double cantilever beam experiments from both printed and unprinted samples

Sample	n	NL Point (J m^{-2})	VIS Point (J m^{-2})	C5%/Max Point (J m^{-2})	Median PROP (J m^{-2})
Unprinted Control	22	329 ± 16	336 ± 15	338 ± 13	331 ± 12
1% M401	12	325 ± 16	334 ± 18	335 ± 17	328 ± 16
5% M401	5	354 ± 22	360 ± 11	363 ± 20	377 ± 21
5% M400	6	360 ± 21	370 ± 19	380 ± 18	420 ± 28

Given error is 1 std. dev. , n = number of specimens in sample average

From the data several aspects are striking: firstly that both 5% printed laminates show higher G_{IC} values and secondly that the
5 1% concentration print doesn't appear to have significantly affected the interlaminar properties. The increase in G_{IC} is most apparent from the mean-median propagation points; this can be attributed towards the fact that these samples appear to more often display a rising trend in G_{IC} against delamination length that
10 is not so apparent in the control samples. As mentioned before such a rising trend is normally attributed to the influence of fibre bridges near the crack tip which increase the rate of critical energy release required to propagate the crack. It is possible that the presence of the patterned polymers at the interface increases
15 G_{IC} by interrupting the process of microcrack coalescence by forcing alternative paths which also produces a fibre bridging effect.

In order to check the statistical significance of these results the difference in means between the different groups was tested
20 using one way analysis of variance (ANOVA). The results of the ANOVA show that the means of the NL points [$F_{(3, 41)} = 8.09$, p = 2.39 x 10^{-4}]; VIS points [$F_{(3, 41)} = 9.26$, p = 8.45 x 10^{-5}]; C5%/MAX points [$F_{(3, 41)} = 14.82$, p = 1.10 x 10^{-5}] and the mean of the median propagation points [$F_{(3, 41)} = 56.70$, p =
25 1.21 x 10^{-14}] are not equivalent as the p values are all significantly smaller than the significance level (0.05).

A post-hoc Tukey test on the groups (at the 0.05 significance level) reveals that both of the 5% printed laminates perform significantly better for all four parameters compared to the
30 control (and the 1%). There is no significant difference between the 5% printed laminates with M400 and M401 in terms of NL point, VIS point and MAX/C5% point but in terms of propagation points M400 performs significantly better. The 1% M401 samples does not differ from the unprinted controls
35 significantly for any of the four parameters.

Evaluating effect of a thermal cycle on the DCB specimens.

From the tested DCB specimens a control sample and both the 5% M401 and 5% M400 printed samples were subjected to a thermal healing cycle. The DCB tests were repeated for the
40 thermally cycled specimens. The aim of the test was to see if there was any rebonding of the previously delaminated specimen faces. Healing, however, was not observed as there was no

noticeable resistance to delamination up until the point where the test had previously been stopped (~5 mm from the end of the
45 specimen). There was also not enough remaining specimen length to get the required data points needed to produce G_{IC} values for the re-initiation of the crack.

The fact that healing was not observed is disappointing but not entirely surprising given the small quantity of material printed
50 between the plies. The test is quite severe as the plies are completely peeled away from each other (and there is no guarantee that perfect contact is re-established during the healing cycle. In order to see any healing at this level much more material is likely to be required.

55 **Composite Testing: Short Beam Shear**

Short beam shear (SBS) testing was performed on four samples: unprinted control, 1% M400, 5% M401 and 5% M400. Typical plots of the apparent interlaminar shear stress against extension are shown for all four samples in Fig. 4 with the particular
60 specimens chosen because they were close to the mean and therefore good representations of the batch.
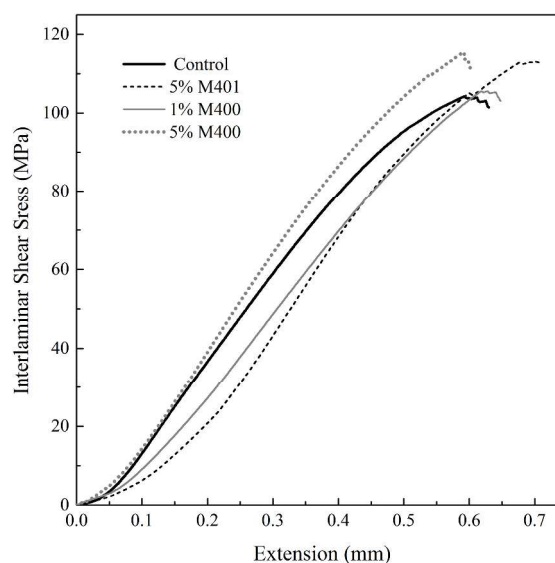

Fig. 4 Four separate typical interlaminar shear stress against extension plots obtained from short beam shear experiments for both printed and
65 unprinted control composite samples.

This journal is © The Royal Society of Chemistry 2014

J. Mater. Chem. A, 2014, **[vol]**, 00–00 | **8**

In the case of both the 5% concentration samples the inner four plies out of a total of eight plies were printed. In the case of the 1% M400 printed sample all plies were printed. The number of specimens produced from each panel was 14; however the specimens that failed obviously in compression or tension were discarded leaving between 7 and 10 specimens from each batch that appeared to fail in single or multiple shear.

The mean results are tabulated in Table 3. A one-way ANOVA [$F(3, 30) = 17.86$, $p = 7.70 \times 10^{-7}$] shows that the means are significantly different at the 0.05 level. Post-hoc analysis with the Tukey test reveals that only the 5% printed samples show a significantly higher apparent interlaminar shear strength compared to the control and the 1% M400 printed samples. There is no significant difference between the two 5% printed specimens and there is no significant difference between the 1% printed specimens and the control despite the 1% specimens having twice as many plies printed.

Table 3 Apparent interlaminar shear strength (aILSS) of the printed and unprinted control composite samples as determined by short-beam method

Sample	n	aILSS (MPa)
Unprinted Control	7	105 ± 2
1% M401 (8 ply printed)	8	106 ± 4
5% M401 (4 ply printed)	9	115 ± 3
5% M400 (4 ply printed)	10	116 ± 3

Given error is 1 std. dev. (n = number of specimens in average)

These results compare favourably with those from the DCB tests. Printing with M400 and M401 at the 5% level clearly has a beneficial effect on the interlaminar properties. Printing at the 1% concentration deposits an amount of material that is too small to have any discernible effect on the properties.

Evaluating effect of a thermal cycle on the SBS specimens.

After testing the SBS specimens were subjected to a thermal healing cycle and then retested. The results are shown Fig. 5A. This shows that no samples exhibited a full recovery in interlaminar shear strength after the thermal treatment. However, the samples printed with 5% M400 and 5% M401 show a smaller reduction in properties compared to the control and the 1% printed specimens.
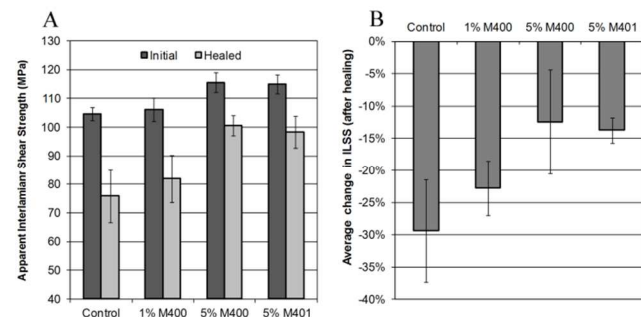

Fig. 5 (A) Apparent interlaminar shear strength (aILSS) results obtained from the short beam method for printed samples and unprinted controls before and after a thermal repair cycle. (B) The average percentage reduction in aILSS after a thermal healing cycle shown for printed and unprinted samples. All error bars shown are 1 std. dev.

On a specimen by specimen basis the percentage decrease in apparent interlaminar shear strength was calculated and the mean results from each sample are shown in Fig. 5B. This shows that the 5% printed specimens showed a smaller percentage reduction in interlaminar properties after a thermal treatment compared to the control. This is consistent with some degree of rebonding of the laminates by the printed polymers.

Comparison with an unprinted control that had also experienced the thermal treatment eliminates the influence of post-cure of the epoxy matrix on the results as this effect (if significant) should be present in all specimens. There is, however, a high degree of uncertainty in this measurement which is likely to come from the variable amount of damage introduced into the specimens during the test. Consequently this result should be considered to be indicative.

Conclusions

Carbon-fibre composite materials are experiencing widespread use in the primary airframes of both civilian and military aircraft. However, there are concerns over the development of barely visible internal damage and delaminations within these composites that may occur over their lifetime and are difficult to detect using conventional non-destructive testing techniques [35]. Interfacial cracks, which are initially small and negligible, can grow until the mechanical performance of a part is severely impaired [36, 37]. These problems are currently addressed by the use of toughened resins and large safety factors which lead to the use of additional material and therefore more weight than would be necessary for a system that was not susceptible to this kind of damage. The work presented in this paper aims to address this problem by providing a mechanism in which these micro delaminations can be repaired using a thermal treatment.

The proposed solution involves inkjet printing of self-healing or toughening polymers between layers on parts (manufactured from prepreg) that are the most susceptible to delamination damage. The main advantage to using inkjet printing is that small concentrations of materials can be applied accurately and consistently using high levels of automation to the areas that need it. The application of small amounts of material to strategically designed locations has the potential to improve properties and safety with a negligible weight gain. The patterns and inks can also be varied to suit the requirements of the part which gives design engineers a good deal of flexibility and control.

The synthesis and development of monomer inks that are suitable for inkjet printing was and a suitable solvent (Ethyl Acetate) was selected which was used to successfully print monomer concentrations of up to 5% onto both prepreg and glass slide substrates. The printed patterns were shown to successfully cure upon thermal treatment without significant spreading.

Printing 5% solutions of M400 and M401 on a single ply at the mid-plane of double cantilever beam specimens was shown to increase the initiation (by NL Point) of the interlaminar fracture toughness by 8% and 9% respectively. The interlaminar fracture toughness with regards to median crack propagation was increased further by 14% and 27% respectively. An application of thermal treatment (under pressure) did not, however, show any evidence of re-bonding the fracture surfaces. Printing of 5% M400 and 5% M400 on the four middle plies of 8-ply samples

produced statistically significant increases in apparent interlaminar shear strength (10% and 11% respectively). After a thermal treatment specimens were retested and it was found that the printed specimens had significantly smaller decreases in properties.

In conclusion, monomers have been synthesised from base chemicals and successfully integrated into aerospace grade composites using the novel technique of inkjet printing. The printing has been shown to have a positive effect on both interlaminar fracture toughness and apparent interlaminar shear strength. In addition there is evidence of self-healing behaviour after retesting of thermally treated short beam shear specimens compared to the control. This is an excellent result which warrants further development.

The tests chosen to demonstrate the self-healing behaviour of the printed patterns are fairly extreme and represent a case of damage far greater than that at which they would be employed in practice. Now that the concept has been proven it would be ideal to show if the healing behaviour can be demonstrated as a lifetime extension in fatigue testing (with periodic thermal treatments). It is highly probable that the self-healing mechanism would be even more effective to slow down the fatigue damage build-up by re-bonding micro delaminations. This sort of testing would allow more confidence in the self-healing.

It would also be useful to investigate higher monomer loadings, either through more concentrated inks or by multiple passes as the amount of material deposited thus far has been extremely small.

The printed pattern was chosen to allow better comparison with other maters printed on the same substrate within the research group [12, 13]. This print pattern could, however, be varied easily and this could lead to enhancements in the composite properties. Care should be taken, however because it is possible that printing too much material or printing continuously could be detrimental to the interlaminar properties. A full interleave, for example might disrupt the transverse bonding between plies as opposed to the local toughening effect produced by small dissimilar molecules. At the time of writing work is being done on the printing of full interleaves in order to answer this question but the results are not yet ready for publication.

Acknowledgements

Notes and references

a Composite Systems Innovation Centre, Department of Materials Science and Engineering, The University of Sheffield, S1 3JD, Sheffield, UK
b Composite Systems Innovation Centre, Department of Mechanical Engineering, The University of Sheffield, S1 3JD, Sheffield, UK
Fax: +44 (0)114 222 7890; Tel: +44 (0)114 222 77 3; E-mail: patrick.smith@sheffield.ac.uk

1 L. Amenabar, F. Lopez and A. Mendikute, *J. Infrared, Millimeter, Terahertz Waves*, 2013, **34**, 152

2 K. Dragan and W. Swiderski, *Acta Physica Polonica A*, 2010, **117**, 878

3 Y-K Zhu, G-Y Tian, R-S Lu and H. Zhang, *Sensors,* 2011, **11**, 7773

4 Y. Wuliang, P. J. Withers, U. Sharma and A. J. Peyton, *IEEE Trans. Instrum. Meas.*, 2009, **58**, 738

5 P. J. Shubel, R. J. Crossley, E. K. G. Boateng and J. R. Hutchinson, *Renewable Energy,* 2013, **51**, 113

6 T. J. Swait, F. R. Jones and S. A. Hayes, *Compos. Sci. Technol.*, 2012, **72**, 1515

7 J. M. Whitney, in *Interlaminar Response of Composite Materials*, ed. N. J. Pagano, Elsevier, Amsterdam, 2012, vol. 1, ch. 4, pp. 162-247

8 M. B. Madec, P. J. Smith, A. Malandraki, N. Wang, J. G. Korvink and S. G. Yeates, *J. Meter. Chem.*, 2010, **20**, 9155

9 P. J. Smith, D-Y Shin, J. E. Stringer, B. Derby and N. Reis, *J. Mater. Sci.*, 2006, **41**, 4153

10 V. Sanchez-Romaguera, M. A. Ziai, O. Dumtoochukwu, S. Barbosa, J. S. R. Wheeler, J. C. Batchelor, E. A. Parker and S. G. Yeates, *J. Mater. Chem. C.*, 2013, **1**, 6395

11 Y. Zhang, C. Tse, D. Rouholamin and P. J. Smith, *Cent. Eur. J. Eng.*, 2012, **2**, 235

12 Y. Zhang, J. Stringer, R. Grainger, P. J. Smith and A. Hodzic, *Phys. Status Solidi RRL*, 2014, **8**, 56

13 Y. Zhang, J. Stringer, R. Grainger, P. J. Smith and A. Hodzic, *J. Compos. Mater.*, 2014, DOI: 10.1177/0021998314533715

14 X. X. Chen, M. A. Dam, K. Ono, A. Mal, H. N. Shen, S. R. Nutt, K. Sheran and F. Wudl, *Science*, 2002, **295**, 1698

15 Y. L. Liu and C. Y. Hsieh, *J. Polym. Sci., Part A: Polym. Chem.*, 2006, **44**, 905

16 Y. L. Liu and Y. W. Chen, *Macromol. Chem. Phys.*, 2007, **208**, 224

17 P. A. Pratama, M. Sharifi, A. M. Peterson, G. R. Palmese, *ACS Appl. Mater. Interfaces*, 2013, **5**, 12425

18 M. R. Kessler, N. R. Sottos and S. R. White, *Composites, Part A*, 2003, **34**, 743

19 R. S. Trask, G. J. Williams and I. P. Bond, *J. R. Soc., Interface*, 2007, **4**, 363

20 J. S. Park, K. Takahashi, Z. Guo, Y. Wang, E. Bolanos, C. Hamann-Schaffner, E. Murphy, F. Wudl and T. H. Hahn, *J. Compos. Mater.*, 2008, **42**, 2869

21 D. A. Hurley and D. R. Huston, *Smart Mater. Struct.*, 2011, **20**, doi:10.1088/0964-1726/20/2/025010

22 E. B. Murphy, E. Bolanos, C. Schaffner-Hamann, F. Wudl, S. R. Nutt and M. L. Auad, *Macromolecules*, 2008, **41**, 5203

23 D. Peters, *J. Chem. Soc.*, 1959, 1761

24 G. L. Dunn and J. K. Donohue, *Tetrahedron Lett.*, **31**, 3485

25 BS ISO 15024, *Fibre-reinforced plastic composites – determination of mode I interlaminar fracture toughness, HIC for unidirectionally reinforced materials*, British Standards International, 2001.

26 BS EN ISO 14130, *Fibre-reinforced plastic composites – Determination of apparent interlaminar shear strength by short-beam method,* British Standards International, 1998.

27 J. Thiele, *Chem. Ber.* 1900, **33,** 666

28 D. Stoye, in *Ullmann's Encyclopedia of Industrial Chemistry,* Wiley-VCH, Weinheim, 2012, Electronic Release, DOI: 10.1002/14356007

29 T. E. Daubert and R. P. Danner, in *Physical and Thermodynamic Properties of Pure Chemicals Data Compilation*, Tayor and Francis, Washington D. C. , 1996

30 J. E. Fromm, *IBM J. Res. Dev.*, 1984, **28**, 322

31 D. Jang, D. Kim and J. Moon, *Langmuir*, 2009, **25**, 2629

32 N. Reis and B. Derby, *MRS Proceedings,* 2000, **625**, DOI: 10.1557/PROC-625-117

33 D. B. van Dam, C. L. Clerc, *Phys. Fluids*, 2004, **16**, 3403

34 J. Perelaer, P. J. Smith, E. van den Bosch, S. S. C. Grootel, P H. J. M. Ketelaars, U. S. Schubert, *Macromol. Chem. Phys.* 2009, **210**, 495

35 P. Kumar and B. Rai, *Compos. Struct.* 1993, **23**, 313

36 A. C. Garg, *Eng. Fract. Mech.* 1988, **29**, 557

37   A. Arguelles, J. Viña, A. F. Canteli and J. Bonhomme, *Polm. Composites*, 2009, **31,** 700

Journal of Materials Chemistry A Accepted Manuscript
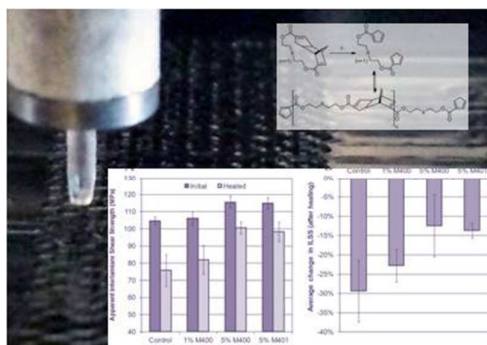
Carbon fibre composites containing discrete inkjet printed monomeric inclusions demonstrate improved interlaminar properties and recovery after damage